

USSR ACADEMY OF SCIENCES  
A.F. IOFFE PHYSICO-TECHNICAL INSTITUTE (ORDER OF LENIN)  
Report 197

CERN LIBRARIES, GENEVA



CM-P00100664

SPECTROMETRIC CHARACTERISTICS OF THE TOTAL ABSORPTION CERENKOV COUNTER  
WITHIN THE NANOSECOND TIME REGION

V.S. Bekrenev, S.P. Kruglov and A.I. Shchetkovskij

Leningrad 1969

Translated at CERN by R. Luther  
(Original: Russian)  
Not revised by the Translation Service

(CERN Trans. 71-11)

Geneva  
March 1971

The background in total absorption spectrometric counters is estimated for given values of the pulse pile-up probability. Methods of constructing electronic recording systems are examined and the main circuits of the basic logical elements are shown. An experimental investigation is made of the spectrometric and time characteristics of the total absorption Cerenkov counter. The value of the counter's energy resolution, determined as the relation of the total width half-height of the pulse distribution curve pulse-height to the maximum varies from 42% to 16% within the msec time region and from 53% to 22% within the nsec time region when the incident electron energy rises from 100 MeV to 600 MeV accordingly. The instrument's efficiency  $\approx 100\%$ .

#### 1. Estimates of tolerable backgrounds.

Considerable distortions may occur in the energy spectra of electrons and  $\gamma$  quanta obtained with the aid of Cerenkov or scintillation spectrometers when there is a heavy background. These distortions may appear as alterations in the shape of the spectral line and as a shift in the maximum of the spectrum investigated.

This is due firstly to the recording of background particles as the result of accidental coincidences, and secondly to the pile-up of pulses from the process under investigation and of background pulses. If the background particles are independently produced, then the number of events in the first case may be determined with the aid of the well-known formula

$$N_{ca} = n N_1 N_2 \dots N_n \tau^{(n-1)}, \quad (1)$$

when  $n$  is the number of coincidence channels,  $N_1$  is the pulse count per channel and  $\tau$  is the resolving time of the coincidence circuit. To estimate the number of pulse pile-ups from the real events and from the background, it is essential to establish the probability of this process for a common background of  $N$  pulses/sec per channel. If the signal gating time to the pulse-height analysis system equals  $\tau_1$ , then the probability  $P(m)$  - the occurrence in this time interval of a number of pulses greater than  $m$  - is determined by the Poisson integral distribution

$$P(m) = \sum_{k=m}^{\infty} \frac{(N \cdot \tau_1)^k}{k!} \exp(-N \tau_1). \quad (2)$$

As pulses from photomultipliers have a certain duration  $\tau_2$ , the probability of the pile-up of real and background signals will be greater than (2). This is equivalent to an increase in the duration of the time interval for examination by the value  $\tau_2$ .  $P(m)$  may then be determined to a sufficient degree of accuracy for practical purposes by means of the formula:

$$P(m \geq 1) = (\tau_1 + \tau_2) N. \quad (3)$$

Thus, for  $N_0$  recorded useful events, the number of distorted pulses will equal:

$$N' = N_0 (\tau_1 + \tau_2) N. \quad (4)$$

Background sources in accelerators may be conditionally split up into two groups:

1) radiation connected with particle scattering inside the accelerator chamber; on the walls of the collimators and on the target casing, in the magnets and on the walls of the experimental hall.

2) radiation caused by competitive reactions where the particle beam interacts with the target material (physical background)

The effect of background events included in the first group is usually cancelled by subtracting spectra obtained with and without the target. The effect of the events of the second group on the background is suppressed by "redetermining" the problem, ie. by measuring a larger number of the reaction's kinematic parameters than is required for a single-valued determination. However, neither of these methods is effective if the particles' energy spectra are substantially distorted by the pile-up of background pulses during the measurement process. Let us take as an example the experiment for determining the mass of an unknown neutral  $X^0$ -meson during the study of the process  $\pi^- p \rightarrow n X^0 \rightarrow 2\gamma$ . Two identical Cerenkov spectrometers are used to measure the energy and emission angles of the  $\gamma$  quanta. The sources of the physical background from the target are the reactions  $\pi^- p \rightarrow n \pi^0 \rightarrow 2\gamma$ ,  $\pi^- p \rightarrow n \pi^+ \pi^- \rightarrow 2\gamma$ ,  $2\gamma$ ,  $\eta^0 n \rightarrow 2\gamma$  etc., and the energies of the background  $\gamma$  quanta equal and even exceed the energies of the  $\gamma$  quanta from the  $X^0$  decays. The effective mass of the unknown particle may be determined by the formula:

$$M_x = (4E_{\gamma_1} E_{\gamma_2} \sin^2 \Psi/2)^{1/2}, \quad (5)$$

where  $E_{\gamma}$  is the energy of the  $\gamma$  quantum,  $\Psi$  is the angle between the  $\gamma$  quanta.

If a pulse pile-up occurs in one of the spectrometers due to background  $\gamma$  quanta with a mean energy  $E = E_\gamma$ , then, in the event of maximum distortion of the pulses under analysis, the particle's measured mass will be  $M = 1.41M_x$  and the relationship between the relative error of the mass and the pile-up probability  $P(m)$  may be determined from the formula:

$$\frac{\Delta M_x}{M_x} = 0,41 P(m). \quad (6)$$

If the maximum systematic error in determining the particle's mass is limited by the value  $\frac{\Delta M_x}{M_x} = 0,01$ , then pile-ups will be tolerable in no more than 2,5% of cases.

A first approximation of the maximum value for background  $N$ , at which distortions do not exceed the tolerable values indicated, may be obtained from formula (3). Fig. 1 shows curves of the dependence of  $N$  for various photomultiplier pulse lengths with a pile-up probability  $P(m) = 0.02$  on the signal gating time to the pulse-height analyzer. As can be seen from the graphs, to ensure the satisfactory operation of the spectrometer when there is a considerable background, it is essential to select photomultipliers with minimum current pulse length and to use "fast" gating circuits. Both these curves and formula (1.4) are based on the assumption that the particles have a uniform time distribution. If the background source is cyclic, as is the case with accelerators, then the  $N$  values are correct for each time interval during which the accelerator completes an operating cycle and in which the particles' time distribution is uniform.

The practical measurement of the background mean value, related to the time interval  $\Delta t = 1$  sec (without allowing for the beam's micro-structure) equals:

$$N_{cp} = NTf, \quad (7)$$

where  $N = P(m) (\tau_1 + \tau_2)$ ,  $T$  is the duration of the accelerator's operating cycle and  $f$  is the cycle repetition rate.

Thus, for values  $T = 1$  msec,  $f = 50$  hz,  $P(m) = 0.02$  and using up-to-date photomultipliers with large-diameter photocathodes whose own current pulse frequency is 40 nsec, the threshold value of the mean background is  $\approx 2 \cdot 10^4$  pulse/sec (instantaneous value  $N \approx 4 \cdot 10^5$  pulse/sec) and it may be achieved by reducing the pulse gating time to the pulse-height analyzer to 10 nsec.

If the gating time  $\tau_1 = 1$  msec, the value  $N_{cp}$  for those parameters is  $\sim 10^3$  pulse/sec. (instantaneous value  $N \approx 2 \cdot 10^4$  pulse/sec).

## 2. Recording systems

The total absorption Cerenkov and scintillation spectrometers used to determine the energies of electrons and  $\gamma$  quanta usually feature the pulse-height analysis of voltage pulses whose value is proportional to the total charge at the photomultiplier's anode. This is done with the aid of the following recording systems.

I. The "slow" system /2/ in which current pulses are integrated at the photomultiplier's output by an  $RC_a$  network where  $R = \frac{R_a R_{bx}}{R_a + R_{bx}}$ , and

$C_a = C_1 + C_2 + C_3$ , where  $C_1$ ,  $C_2$  and  $C_3$  are the capacitances of the photomultiplier's anode, the wiring and the pre-amplifier's input stage respectively (fig, 2a). To reduce distortion during integration, value  $R_a$  is of the order of hundreds of kilohms, giving a voltage pulse decay time of several microseconds. The time selection of events is done by putting the spectrometer in coincidence with scintillation counters or with another spectrometer. For instantaneous background values not exceeding  $10^4$  pulse/sec, the spectrometer's energy resolution is in fact governed only by the statistical processes occurring in the radiator and photomultipliers.

Shortcomings of the system:

- a) considerable time for the accumulation of voltage pulses at the photomultiplier's output, determined by the duration of the current pulses;
- b) the need for the inclusion of special circuits in the spectrometer itself in order to match the photomultiplier's high output resistance with the cable's wave impedance;
- c) the possibility of overloading the first stages of the input device.
- d) the low value for threshold background.

II. The "fast" system [3,4], in which the photomultiplier's load resistance value is selected so that the time constant  $R_a C_a$  is much less than the rise time for the current pulse. In this case the integrating effect of the photomultiplier's anode capacitance has virtually no influence on the shape of the signal and the voltage pulse, which is similar in shape to the current pulse, branches out into two channels: time and spectrometric. In the first channel a control pulse is shaped which then goes into the

coincidence circuit; in the second channel, after the linear gating device, the pulse is integrated by a special circuit. As the electronic recording apparatus is normally situated a considerable distance from the spectrometer and is connected to the latter by an HF cable, the photomultiplier's load resistance equals the cable's wave impedance (fig. 2b).

In such a system the rise time and the duration of output pulses from photomultipliers for plastic and Cerenkov radiators are determined solely by the time properties of the photomultiplier as the de-excitation time of these radiators is  $\sim 10^{-9}$  sec.

If the voltage pulse coming from the photomultiplier for examination is fully enclosed by the gate to the integrating device and the pulse-height analyser, the value for the spectrometer's energy resolution will be the same for both "fast" and "slow" systems. If the gating time is less than the signal length, i.e. it is cut off, then the height of the voltage pulses reaching the analyzer will be proportional to the photomultiplier's current pulses which have a considerable height spread due to the time fluctuations: this decreases the device's resolution. With this recording system it is possible to improve the spectrometer's time properties substantially and to increase the ultimate background by more than 10 times compared with (1).

III "fast-slow" system, in which the control signal for the coincidence circuit is shaped by time photomultipliers, and a conventional "slow" recording system determines the particles' energy using spectrometric photomultipliers. By using coincidence circuits with a resolving time of



$10^{-8}$  sec, it is possible to reduce the number of random events considerably in comparison with I, but as spectrum distortion depends basically on the length of the output pulses from spectrometric photomultipliers, the tolerable background for this system will be less than for II. Moreover, to obtain an adequate energy resolution in a Cerenkov spectrometer, a large part of the visible light created by the particles in the radiator must fall on the cathodes of the spectrometric photomultipliers. In this connection, the amount of light quanta incident on the cathodes of the time photomultipliers forms only a small fraction of their total number: this reduces the efficiency of the device at particle energies  $< 200$  MeV because of the low overall intensity of the Cerenkov light in the radiator and the big fluctuations in the showers.

This paper contains a study of the energy characteristics of the total absorption Cerenkov spectrometer using "slow" and "fast" recording systems. In addition, the efficiency of the detector for the "fast" system was measured in relation to coincidences from two scintillation counters.

### 3. Design of a Cerenkov counter

TF-1 lead glass was used as a Cerenkov light radiator in the counter: it had the following characteristics:  $n = 1.65$ ,  $\rho = 3.86$  g/cm<sup>3</sup>,  $d = 2.38$  cm. Two identical rectangular glass blocks formed a parallelepiped measuring 350 x 300 x 300 mm<sup>3</sup> which was scanned at one end by 4 F.E.U.-49 photomultipliers. The diameter of the working section of the F.E.U. photocathodes

was 155 mm. The glass blocks were located in a housing consisting of two rectangular pieces of steel, the walls of which were 5 mm. thick. The blocks were light-sealed and formed two virtually independent radiators. All their surfaces were polished and their facets covered with aluminium foil to improve light collection. Optical contact between the radiator and the photocathodes was ensured by means of a silicon paste. The value of the photocathodes' quantum sensitivity for each photo-multiplier was not less than 190 microamp/lumen; the current pulse rise time when the photocathodes were illuminated by nanosecond light pulses was 16 nsec; and the total pulse length was  $40 \pm 5$  nsec.

#### 4. Electronics

The block diagram of the "slow" recording system is shown in fig. 3. Voltage pulses from the photomultipliers' load resistances ( $R = 270$  kilohm) passed through the White cathode followers into the fan-in circuit which comprises a cascode amplifier containing 4 input valves  $L_5 - L_8$  with one valve  $L_9$  as a load connected via the circuit to the overall network. The variable transfer coefficient for each of the instrument's channels enabled the pulse heights from the different photomultipliers to be matched without altering their supply voltages. A positive polarity output signal with anode loading was gated from valve  $L_9$  through a matched cable to the U.I.S.-2 linear amplifier. Pulse-height analysis was done by a 100-channel AI-100-1 analyzer, operating in a coincidence mode. The control pulse was generated by a special circuit, triggered by a

The energy of the collimated monochromatic particle beam varied within the range 100 ÷ 600 MeV with a maximum pulse instability of 1.5%. The operating voltage of the spectrometer's photomultipliers remained constant throughout the measurements and their sensitivity was balanced with the aid of light from a gallium phosphide diode to which voltage pulses of standard height were sent.

Fig. 12 shows the shape of the spectrum lines for various energies of primary particles. As the curve shapes are close to normal in virtually every case, the detector's resolution was found by approximating these curves using the Gauss function: the standard deviation  $\sigma$ , the pulse height at maximum  $A$  and the value  $\chi^2$  were also calculated. The device's resolution value  $\delta$ , determined as the relation of the total width half-height of the pulse height distribution curve to the maximum height, was found from the relationship

$$\delta = 2\sqrt{2\ln 2} \frac{\sigma}{A} \quad (8)$$

Fig. 13 shows firstly the dependences of the spectrometer's resolution on the energy of bombarding electrons and secondly the pulse height characteristics for the "fast" and "slow" recording systems. The pulse gating times selected were 25 nsec. and 4 microsec.

As the graphs show, the detector's resolution value drops regularly when only parts of a pulse are gated to the pulse-height

non-linear at 0.8V (at the output) because of the double diode limiting of the signals and the cut-off of the D.C. current from transistor  $T_2$ . The input and output pulses have negative polarity.

The considerable gain of the whole time channel combined with the good loading properties made it possible to feed pulses of standardized height into the coincidence circuit with a faster rise time.

The linear gating circuit has a diode bridge which is controlled by pulses of opposite polarities /6/. Control by the gate is used for triple coincidences (from two scintillation counters and the spectrometer); minimum pulse gating time  $\approx 25$  nsec.

The main circuit of the integrating amplifier is shown in fig. 10. The time constant for integration by the amplifier  $> 1$  microsecond. Positive polarity output pulses decrease exponentially when the time constant  $\approx 1.5$  microsec. The amplitude performance of circuits for various lengths of square input pulse is shown in fig. 11.

## 5. Experimental Research

Research into the characteristics of the spectrometer was carried out on the auxiliary electron beam of the 650 MeV synchrotron at F.I.A.H. in the USSR.

coincidence signal from two scintillation counters, with crystals  $60 \times 60 \times 10 \text{ mm}^3$  placed in front of the spectrometer's radiator. The coincidence circuits resolving time is  $\sim 10^{-8}$  sec.

The block diagram of the "fast" recording system is shown in fig. 5. Current pulses with load resistances of 75 ohm are gated from the four photomultipliers along a matched cable to a linear fan-in circuit (fig.6). Attenuators with a constant input resistance of 75 ohms were installed in order to balance the sensitivity of each channel in the circuit when the photomultipliers were provided with a fixed supply voltage. Summation of the input signals was achieved by means of the current at the resistance  $R_{14} = 100$  ohms. The circuit's gain per channel is 2, the amplitude response is linear up to 2 volts (at the output) at a resistance of 75 ohms (fig. 7, curve 2). The rise time for a square pulse  $< \text{nsec.}$ , input and output pulses having negative polarity.

The linear amplifier (fig. 8) has a 2-stage loop with complex negative feedback. A variable attenuator with a 75 ohm input resistance is placed at the loop's input. The circuit's gain is 10, the rise time for a square pulse  $< 8$  nsec. and the amplitude response is linear up to 7.5 V (at the output) at a resistance of 75 ohms (fig.7, curve 1). The negative polarity output signal was branched into the integrating amplifier and the pulse-shaping circuit for a temporary selection of events: that circuit consisted of a similar two-stage loop and amplifier-limiter circuit. The latter's amplitude response is extremely

analyzer ( $\tau_i = 25$  nsec.), whilst the overall shape of the curves is determined by the dependence  $I/\sqrt{N_0}$ , where  $N_0$  is the number of converted photoelectrons. In both cases, the pulse-height characteristics are linear throughout the energy range investigated, thus indicating the linear mode of operation of the electronic apparatus, as when the energy of the bombarding electrons is  $E = 100 \div 600$  MeV, the shower is almost totally absorbed by the spectrometer's radiator ( $L = 14$  radian units). The slope of the pulse-height characteristics towards the axis of the abscissae is determined by the pulse gating time to the radiator and the time constant for integration, which is different for the "fast" and "slow" systems.

In order to estimate the error in the calculation of the device's resolution value by the "fast" recording system's apparatus, a measurement was made of the dependence of  $\delta$  on the gate-width of the pulse being examined to the pulse-height analyzer for primary electron energies of  $E = 600$  MeV (fig. 14). As the graphs show, the height of the integrated pulse increases with the gating time and the resolution improves. However, the value  $\delta$  does not drop below 18% whilst the spectrometer's resolution in the case of the "slow" recording system with 600 MeV electrons reaches 16%. This discrepancy can be explained by the poor operation of the pulse-height analyzer's input system, whose transients last much longer than the rise time of the pulses for examination. The dependence of the pulse-height's mean value on the gating time gives grounds to assume that there is a decay time of up to 100 nsec. That

may be caused by a lack of care in the selection of the operating conditions for the photomultipliers and by time delays between them.

The spectrometer's efficiency  $\eta$  when using the "fast" recording system was determined as the ratio of the number of triple coincidences (two scintillation counters and a electrometer) to the number of coincidences from two scintillation counters whose efficiency was taken to be 1.

Fig. 15 shows the dependence of  $\eta$  on the primary electron energy and it can be seen that in the 100-600 MeV range, the spectrometer's efficiency is virtually 100 %: this means that the detector can be used in time selection logical circuits with a resolution  $\sim 10^{-8}$  sec.

#### Conclusion

Thus, the total absorption Cerenkov counter which has been built may be used in physics experiments as a high-energy electron and  $\gamma$ -quantum spectrometer with a resolution varying from 42% to 16% in the microsecond time range and from 53% to 22% in the nanosecond range when the energy of the bombarding particles varies accordingly from 100 MeV to 600 MeV. The device's time properties ensure virtually 100% efficiency for coincidence work with a resolution  $\tau = 10^{-8}$  sec. If the instantaneous background values do not exceed  $10^5$  particles per second, then it is reasonable to increase pulse gating time to the pulse-height analysis system up to the value for the photomultiplier's signal length thus improving the detector's resolution without any great distortion of the energy spectra and without affecting the time characteristics.

The authors wish to thank V.A. Petukhov, M.G. Sedov, V.F. Grushin, E.M. Leykin, M.N. Yakimenko, A.S. Denisov and D.L. Nikolaev for helping with the research work.

REFERENCES

- 1) Yu.K. Akimov, Scintillation methods for recording high-energy particles, Izd. Moscow State University, 56 (1963).
- 2) V.S. Pantuev, M.N. Khachatryan and I.V. Chuvilo, Pribory Tekh. Eksper. 1, 19-21 (1960).
- 3) V.S. Pantuev and M.N. Khachatryan, Pribory Tekh. Eksper. 6, 29 (1963).
- 4) H. Ruderman et al., Report CTBL-81, Pasadena, Calif., 1962.
- 5) Yu.A. Alexandrov et al., Pribory Tekh. Eksper. 5, 45-47 (1965).
- 6) K.B. Keller, Rev. Sci. Instrum., 35, 10, 1360 (1964).



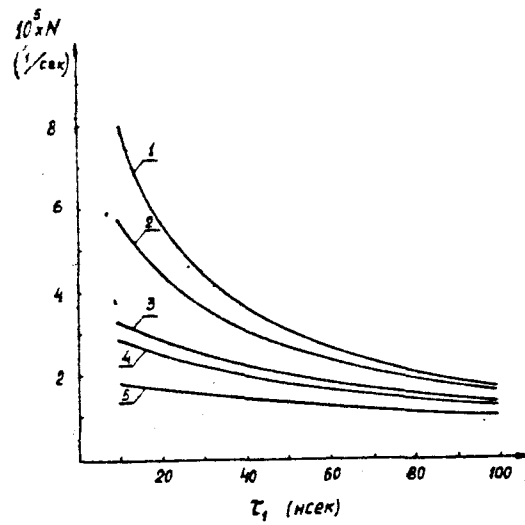


Fig. 1 Dependence of the tolerable background value  $N$  for various pulse lengths  $\tau_2$  from the photomultiplier on the gating time value  $\tau_1$ . The pile-up probability  $P(m) = 0.02$ :

- 1 - ( $\tau_2 = 15$  nsec);    2 - ( $\tau_2 = 25$  nsec);  
 3 - ( $\tau_2 = 50$  nsec);    4 - ( $\tau_2 = 60$  nsec);  
 5 - ( $\tau_2 = 100$  nsec).

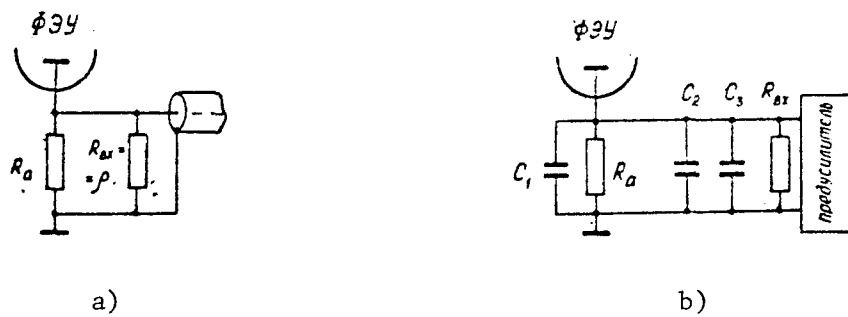


Fig. 2 Wiring diagrams of the photomultipliers:

- a) "slow" system  
 b) "fast" system

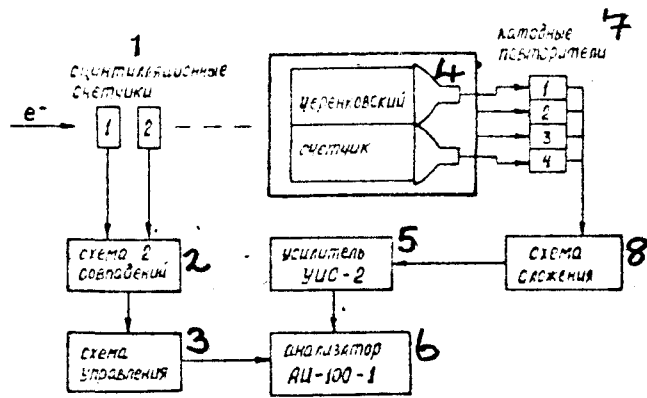


Fig. 3 Block diagram of the "slow" recording system

- |                            |                       |
|----------------------------|-----------------------|
| 1 - Scintillation counters | 5 - UIS-2 amplifier   |
| 2 - 2-coincidence circuit  | 6 - AI-100-1 analyser |
| 3 - Control circuit        | 7 - Cathode followers |
| 4 - Cerenkov counter       | 8 - Fan-in circuit    |

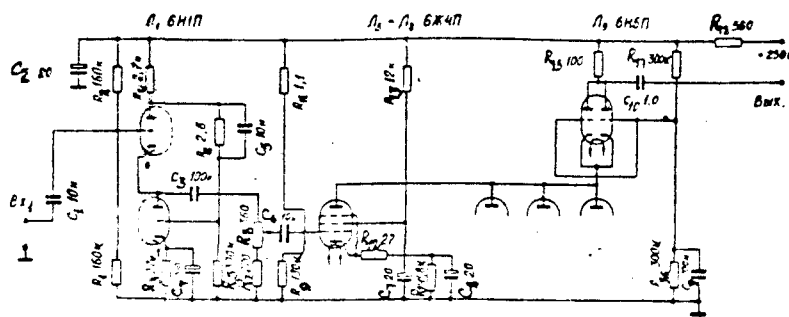


Fig. 4 Microsecond pulse fan-in circuit

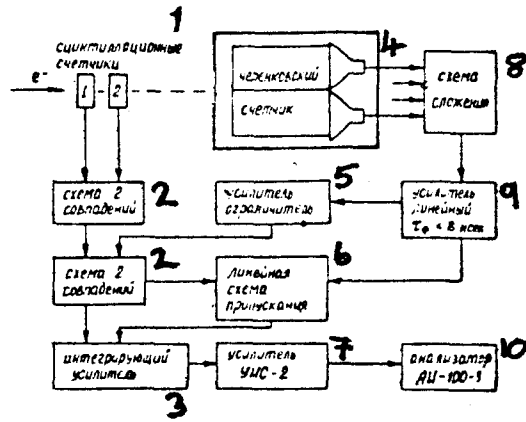


Fig. 5 Block diagram of "fast" recording system

- |                            |                                        |
|----------------------------|----------------------------------------|
| 1 - Scintillation counters | 5 - Amplifier limiter                  |
| 2 - 2-coincidence circuit  | 7 - UIS-2 amplifier                    |
| 3 - Integrating amplifier  | 8 - Fan-in circuit                     |
| 4 - Cerenkov counter       | 9 - Linear amplifier $\tau_0 < 8$ nsec |
| 6 - Linear gating circuit  | 10 - AI-100-1 analyser                 |

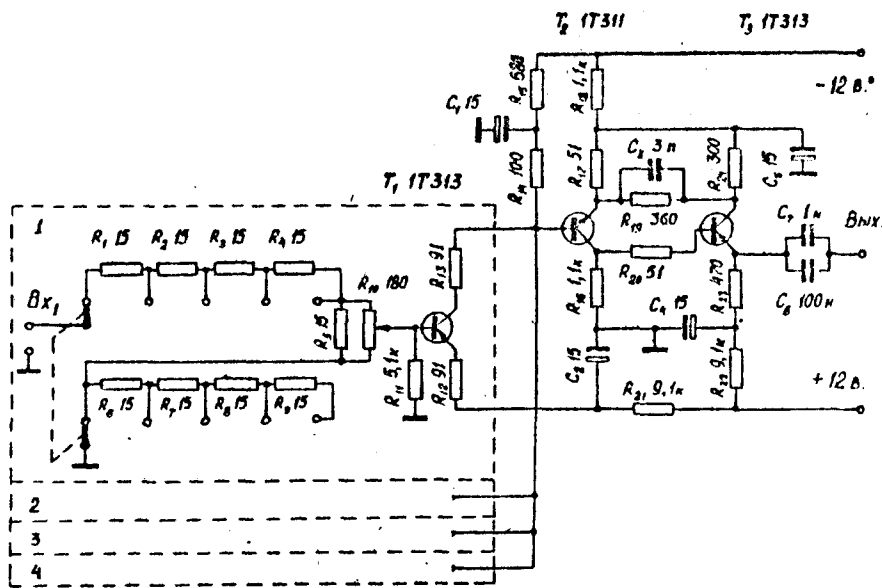


Fig. 6 Fan-in circuit for pulses in the nanosecond range

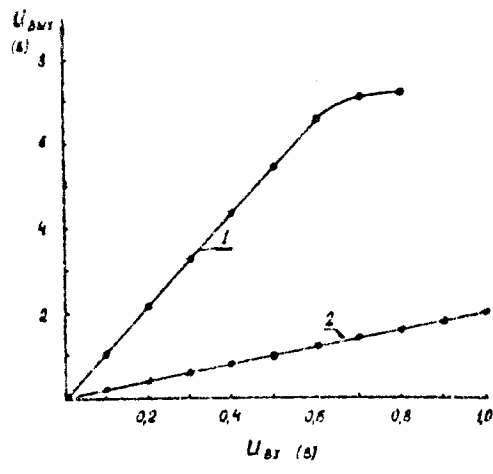


Fig. 7 Pulse-height characteristics  
 1 - Linear amplifier  
 2 - Fan-in circuit

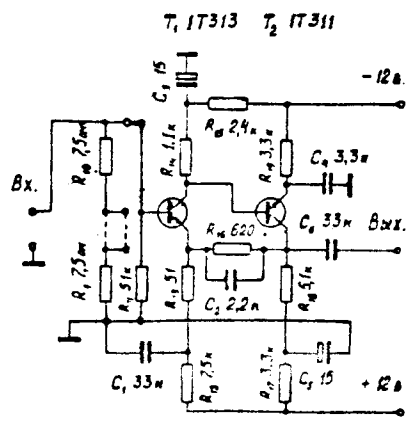


Fig. 8 Linear amplifier circuit

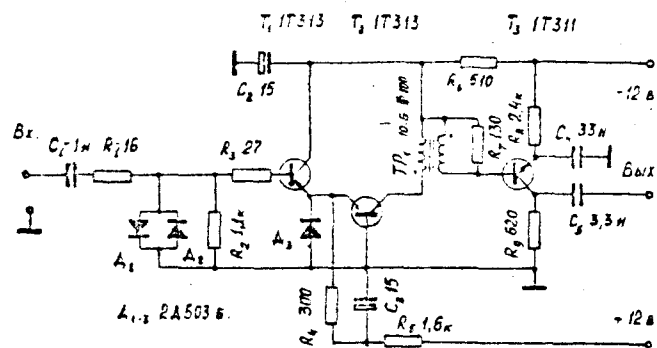


Fig. 9 Amplifier-limiter circuit

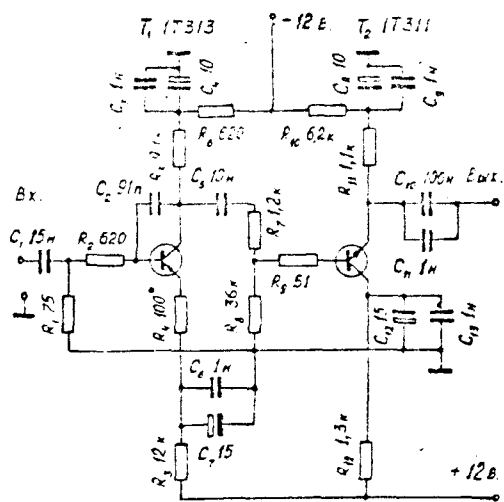


Fig. 10 Circuit of integrating amplifier

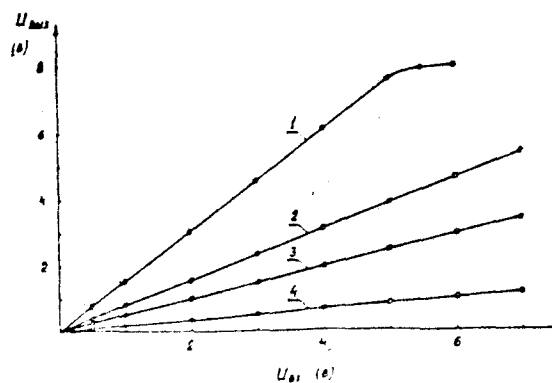


Fig. 11 Pulse-height characteristics of integrating amplifier for various square (input) pulse lengths  $t$ :

- 1 -  $t = 100$  nsec;    2 -  $t = 50$  nsec
- 3 -  $t = 30$  nsec;    4 -  $t = 10$  nsec

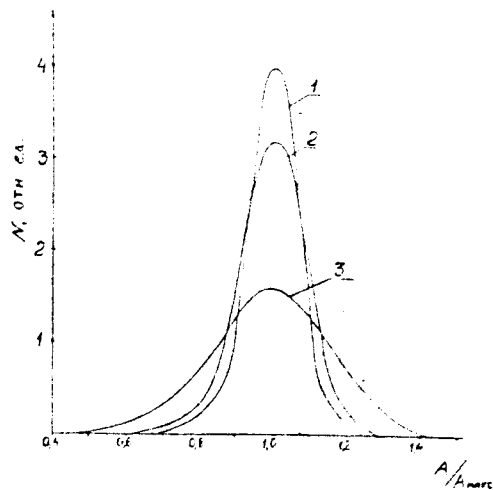


Fig. 12 Spectrometer line shapes

1 -  $E = 600$  MeV; 2 -  $E = 370$  MeV; 3 -  $E = 100$  MeV

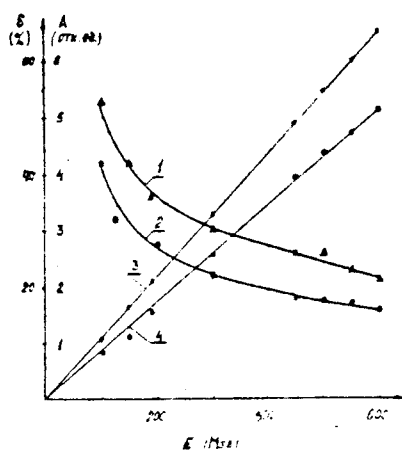


Fig. 13 Dependence of spectrometer resolution  $\delta$  on primary electron energy  $E$ :

1 - "fast" system (gating time 25 nsec)

2 - "slow" system (gating time 4  $\mu$ sec)

Dependence of pulse height at the top of the A-pulse distribution curve on primary electron energy  $E$ :

3 - "slow" system; 4 - "fast" system

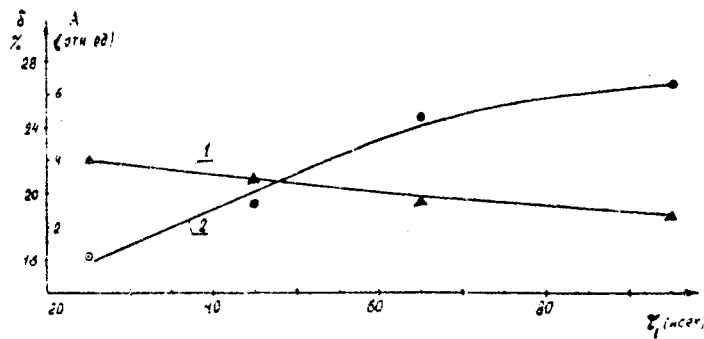


Fig. 14 Dependence of spectrometer resolution  $\delta$  on pulse gating time to the analyser using 600 MeV bombarding electrons (curve 1). Dependence of pulse height at the top of the distribution curve on pulse gating time,  $E = 600$  MeV (curve 2).

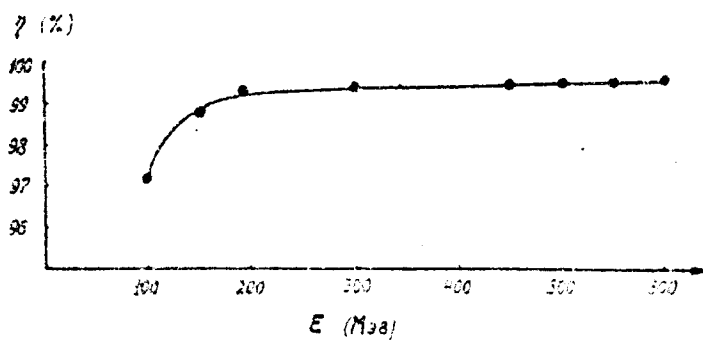


Fig. 15 Dependence of spectrometer efficiency  $\eta$  on primary electron energy  $E$ .